1682 *Inorg. Chem.* **2011**, *50*, 1682–1688
DOI: 10.1021/ic1021609

Inorganic Chemistry
Article

Molecule-Ion Interaction and Its Effect on Electrostatic Interaction in the System of Copper Chloride and β-Cyclodextrin

Le Xin Song,* Jing Yang, Lei Bai, Fang Yun Du, Jie Chen, and Mang Wang

Department of Chemistry, University of Science and Technology of China, Hefei 230026, P.R. China

Received October 27, 2010

The present work was devoted to an experimental investigation of the molecule-ion interaction between copper chloride ($CuCl_2$) and β-cyclodextrin (CD) and its effect on the electrostatic interaction between Cu^{2+} and Cl^- ions. Our results gave an explicit description of the mutual effect between the interactions. First, the molecular arrangement and surface feature of β-CD experienced a fundamental structural change after interaction with Cu^{2+} and Cl^- ions, which was ascribed to a good separation of Cu^{2+} from Cl^- ions in β-CD matrix. Second, arguments based on electronic structural analysis provided a direct indication of the change in charge density distributions of Cu^{2+} and Cl^- ions in the presence of β-CD. Third, the actual occurrence of a second signal in the course of water release at a higher temperature suggested that the Cu^{2+} ions were trapped in the form of hydrates in the crystal interstice of β-CD molecules. Fourth, comparison of the mass spectra indicated that the thermal decomposition of β-CD in the presence of $CuCl_2$ produced a series of interesting molecular ions: $C_3H_2OH^+$, $C_4H_3OH^+$, $C_5H_4OH^+$, and $C_7H_6OH^+$. We consider that this study is helpful in providing a new approach to the evaluation of the extent of the mutual effect between an inorganic salt and an organic molecule.

Introduction

β-Cyclodextrin (CD) is an important representative of cyclic carbohydrates.[1−8] Numerous studies have examined the inclusion interactions between β-CD and hydrophobic guests such as organic molecules, polymers, and organic metal complexes.[9−15] Also, the interactions between β-CD and transition metal cations, such as Cu(II), Pb(II), Cd(II) ions and so on, in alkaline solutions were reported.[4,16−21] Further, Ribeiro and his collaborators found that the interaction between copper(II) chloride ($CuCl_2$) and β-CD in aqueous solutions produced significant effects on electrical conductivity.[22] Furthermore, β-CD can form crystalline coordination compounds with Cu^{2+} ions in alkaline solutions, where the Cu^{2+} ions are in direct contact with the hydroxyl oxygen atoms on the β-CD molecules, and located in the intermolecular space between the β-CD molecules.[23−25] X-ray crystallographic analysis indicated that the Cu^{2+} ion in

*To whom correspondence should be addressed. E-mail: solexin@ustc.edu.cn.

(1) Anibarro, M.; Gessler, K.; Uson, I.; Sheldrick, G. M.; Harata, K.; Uekama, K.; Hirayama, F.; Abe, Y.; Saenger, W. *J. Am. Chem. Soc.* **2001**, *123*, 11854–11862.
(2) Hubert, C.; Denicourt-Nowicki, A.; Roucoux, A.; Landy, D.; Leger, B.; Crowyn, G.; Monflier, E. *Chem. Commun.* **2009**, 1228–1230.
(3) Liu, L.; Guo, Q. X. *J. Phys. Chem. B* **1999**, *103*, 3461–3467.
(4) Norkus, E.; Grinciene, G.; Vuorinen, T.; Vaitkus, R. *J. Incl. Phenom. Macrocycl. Chem.* **2004**, *48*, 147–150.
(5) Caron, L.; Bricout, H.; Tilloy, S.; Ponchel, A.; Landy, D.; Fourmentin, S.; Monflier, E. *Adv. Synth. Catal.* **2004**, *346*, 1449–1456.
(6) Krause-Heuer, A. M.; Wheate, N. J.; Tilby, M. J.; Pearson, D. G.; Ottley, C. J.; Aldrich-Wright, J. R. *Inorg. Chem.* **2008**, *47*, 6880–6888.
(7) Liu, L.; Guo, Q. X. *J. Incl. Phenom. Macrocycl. Chem.* **2004**, *50*, 95–103.
(8) Song, L. X.; Bai, L.; Xu, X. M.; He, J.; Pan, S. Z. *Coord. Chem. Rev.* **2009**, *253*, 1276–1284.
(9) Singh, R. B.; Mahanta, S.; Guchhait, N. *J. Mol. Struct.* **2010**, *963*, 92–97.
(10) Appell, M.; Jackson, M. A. *J. Incl. Phenom. Macrocycl. Chem.* **2010**, *68*, 117–122.
(11) Braga, S. S.; Ferreira, R. A. S.; Goncalves, I. S.; Pillinger, M.; Rocha, J.; Teixeira-Dias, J. J. C.; Carlos, L. D. *J. Phys. Chem. B* **2002**, *106*, 11430–11437.
(12) Yang, Y. W.; Chen, Y.; Liu, Y. *Inorg. Chem.* **2006**, *45*, 3014–3022.
(13) Braga, S. S.; Goncalves, I. S.; Herdtweck, E.; Teixeira-Dias, J. J. C. *New J. Chem.* **2003**, *27*, 597–601.
(14) Braga, S. S.; Gago, S.; Seixas, J. D.; Valente, A. A.; Pillinger, M.; Santos, T. M.; Goncalves, I. S.; Romao, C. C. *Inorg. Chim. Acta* **2006**, *359*, 4757–4764.
(15) Song, L. X.; Du, F. Y.; Guo, X. Q.; Pan, S. Z. *J. Phys. Chem. B* **2010**, *114*, 1738–1744.
(16) Matsui, Y.; Kurita, T.; Yagi, M.; Okayama, T.; Mochida, K.; Date, Y. *Bull. Chem. Soc. Jpn.* **1975**, *48*, 2187–2191.
(17) Matsui, Y.; Kurita, T.; Date, Y. *Bull. Chem. Soc. Jpn.* **1972**, *45*, 3229–3229.
(18) Norkus, E.; Grinciene, G.; Vaitkus, R. *Carbohydr. Res.* **2002**, *337*, 1657–1661.
(19) Norkus, E.; Grinciene, G.; Vuorinen, T.; Vaitkus, R.; Butkus, E. *Int. J. Biol. Macromol.* **2003**, *33*, 251–254.
(20) Fatin-Rouge, N.; Bunzli, J. C. G. *Inorg. Chim. Acta* **1999**, *293*, 53–60.
(21) Li, S. L.; Lan, Y. Q.; Ma, J. F.; Yang, J.; Zhang, M.; Su, Z. M. *Inorg. Chem.* **2008**, *47*, 2931–2933.
(22) Ribeiro, A. C. F.; Esteso, M. A.; Lobo, V. M. M.; Valente, A. J. M.; Simoes, S. M. M.; Sobral, A. J. F. N. *J. Carbohydr. Chem.* **2006**, *25*, 173–185.
(23) Rizzarelli, E.; Vecchio, G. *Coordin. Chem. Rev.* **1999**, *188*, 343–364.
(24) Norkus, E. *J. Incl. Phenom. Macrocycl. Chem.* **2009**, *65*, 237–248.
(25) Harata, K. *Chem. Rev.* **1998**, *98*, 1803–1827.

Published on Web 01/18/2011

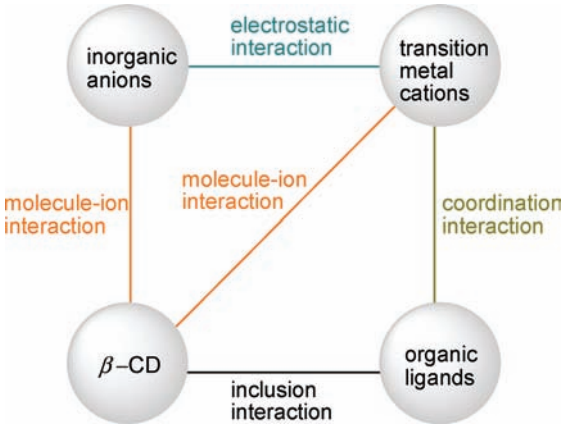

Figure 1. Schematical feature depicting several interactions in a multicomponent system.

the complex $CuCl_2(H_2O)_2$ formed in neutral aqueous solutions tended to stay at the bottom of the primary hydroxyl side of β-CD.[26] Despite the presence of an interaction between β-CD and Cu^{2+} ion or its complexes, the existing studies fall far short of providing practical guidance for understanding how inorganic ions in close-packed structure can be separated by organic molecules.

In recent work, we found that there is an adduct interaction between β-CD and inorganic salts, such as lithium carbonate, sodium arsenite, and ammonium molybdate tetrahydrate.[27−29] And the adduct interaction led to striking changes in spectral properties and thermal stabilities of β-CD and the inorganic salts. Therefore, in considering the d-electron configuration, coordinating ability, and hydratability of transition metal ions, it is interesting and valuable to investigate the presence of the molecule-ion interaction between β-CD and transition metal ions. As shown in Figure 1, this may allow us not only to detect what the mutual effect is between molecule-ion interactions and electrostatic interactions but also to trace the relationship among molecule-ion interactions, inclusion interactions, and coordination interactions. The present work was focused on the former aspect, that is, molecule-ion interaction and its effect on electrostatic interaction.

According to this point of view, initially, we prepared a solid adduct of $CuCl_2$ and β-CD, and characterized the molecular arrangement and surface structure of the molecule-ion adduct. Next, the electronic structure of the Cu^{2+} ion in the adduct was compared with that of free state. And then, the thermal decomposition process and decomposition products were discussed.

Our results gave strong evidence that there was a molecule-ion interaction between β-CD and Cu^{2+} ions as well as Cl^- ions, which is in good agreement with the result obtained in solution.[22] In particular, the molecule-ion interaction had caused a significant effect on the electrostatic interaction between Cu^{2+} and Cl^- ions. We consider that this study would be helpful to bridge the gap between the molecule-ion interaction of β-CD with inorganic ions and the electrostatic interaction of the cation with anion entities.

(26) Kurokawa, G.; Sekii, M.; Ishida, T.; Nogami, T. *Supramol. Chem.* **2004**, *16*, 381–384.
(27) Song, L. X.; Bai, L. *J. Phys. Chem. B* **2009**, *113*, 9035–9040.
(28) Song, L. X.; Dang, Z. *J. Phys. Chem. B* **2009**, *113*, 4998–5000.
(29) Song, L. X.; Wang, M.; Dang, Z.; Du, F. Y. *J. Phys. Chem. B* **2009**, *114*, 3404–3410.

Experimental Section

Materials. β-CD was purchased from Shanghai Chemical Reagent Company and recrystallized twice from deionized water. $CuCl_2\cdot 2H_2O$ was obtained from Guangdong Xilong Chemical Reagent Company and used as received without further purification. All other chemicals were of general-purpose reagent grade, unless otherwise stated.

Preparation of Solid Samples. One mmol β-CD (1.135 g) and 1 mmol $CuCl_2\cdot 2H_2O$ (0.170 g) were resolved in 120 mL deionized water, and stirred for 6 h at 333.2 K in a round-bottom flask. After solvent was removed by rotary evaporation below 323.2 K, a green product ($CuCl_2-\beta$-CD) was obtained in this manner. After drying in air, the crude product in the form of crystal powder was further dried at 333.2 K for 2 h to remove water molecules from the solid, and kept in a vacuum desiccator until further use. Fourier transform infrared (FTIR) data of the adduct $CuCl_2-\beta$-CD: 3425, υ_{O-H}; 1420, δ_{O-H}; 1157, 1080, 1030, υ_{C-O}; 945 cm^{-1}, υ_{C-O-C}. The physical mixture of β-CD and $CuCl_2\cdot 2H_2O$ was prepared by mixing equimolar amounts of the two compounds in a mortar. One mmol of $CuCl_2\cdot 2H_2O$ (0.170 g) were first pulverized for 10 min by hand in a mortar, and then added to powdered β-CD (1 mmol, 1.135 g) and mixed 15 min.

Sintering Experiments. A small amount of samples of β-CD, $CuCl_2\cdot 2H_2O$, and their adduct were dried to be of constant weight at 333.2 K under vacuum (76 Torr). After cooled to 298.2 K in evacuated desiccators over P_2O_5, all the samples were weighed and calcined at 523.2, 573.2, 623.2, 673.2, and 723.2 K for 2 h under ambient atmosphere in a muffle furnace. Each residue was cooled to 298.2 K in a desiccator and then weighed.

Instruments and Methods. X-ray diffraction (XRD) analyses of solid samples were carried out in a Philips X'Pert Pro X-ray diffractometer. Samples were irradiated with monochromatized Cu Kα and analyzed in the 2θ range from 5 to 40°. Tube voltage and current were 40 kV and 40 mA, respectively. FTIR spectroscopy was recorded in a Bruker Equinox 55 spectrometer with KBr pellets in the range of 4000−400 cm^{-1} with a resolution of 4 cm^{-1}. Crystal morphologies of β-CD and $CuCl_2-\beta$-CD were characterized using a Supra 40 field emission scanning electron microscope (FE-SEM) operated at 5 kV. Raman spectra were measured in the range of 90−1800 cm^{-1} with a LABRAM-HR Confocal Laser MicroRaman spectrometer with a resolution of 0.6 cm^{-1} at room temperature.

Room-temperature electron spin resonance (ESR) spectra were recorded at X-band (9.065 GHz) on a JEOL JES-FA200 ESR spectrometer. Microware power employed here was 0.998 mW, and sweep width was 2000 Hz. Modulation frequency and modulation amplitude were 100 kHz and 3 G, respectively. X-ray photoelectron spectroscopy (XPS) was performed at Photoemission Station of National Synchrotron Radiation Laboratory of Hefei with a VG Scienta R3000 electron energy analyzer, using Al Kα radiation (1486.6 eV) in ultrahigh vacuum (2.00×10^{-9} Torr) at room temperature. The energy resolution of the instrument is 0.16 eV. The C1s peak (284.8 eV) was used as the internal standard for binding-energy calibration.

Thermogravimetric/differential thermogravimetric analyses (TG/DTG) were obtained on a Shimadzu TGA-50 thermogravimetric analyzer at a heating rate of 10.0 K·min^{-1} under a nitrogen atmosphere with a gas flow of 25 mL·min^{-1}. Gas chromatography−time-of-flight−mass spectrometry (GC-TOF-MS) experiments were done with a Micromass GCT-MS spectrometer by the aid of a programmed control device.[30]

Results and Discussion

Microstructural Analysis. The comparison of Figures 2a−d brings out a striking change taking place in the present interaction system consisting of $CuCl_2\cdot 2H_2O$ and

(30) Song, L. X.; Xu, P. *J. Phys. Chem. A* **2008**, *112*, 11341–11348.

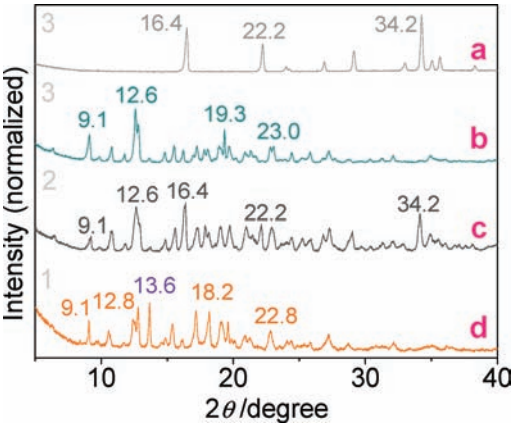

Figure 2. XRD patterns of $CuCl_2 \cdot 2H_2O$ (a), β-CD (b), the physical mixture (c), and $CuCl_2-\beta$-CD (d). Relative signal intensity was normalized to the intensity of the peak at 13.6° in curve d.

β-CD. The major feature of the change is that the three strong peaks of $CuCl_2 \cdot 2H_2O$[31] at 2θ angles of 16.4 (110), 22.2 (020), and 34.2° (121) disappear in the case of $CuCl_2-\beta$-CD but remain in the physical mixture. Also, the strong peaks of β-CD[29] at 12.6 (111), 19.3 (410), and 23.0° are altered in different ways or to different degrees in the case of the $CuCl_2-\beta$-CD, but these peaks as well as 9.1° (101) almost do not change in the case of the physical mixture except for the peak at 19.3°.

Importantly, there is a new strong peak centered at 13.6° (*d*-spacing, 0.651 nm) occurring in the $CuCl_2-\beta$-CD. This situation does not happen in the physical mixture. The appearance of the new peak may suggest the intercalation of Cu^{2+} and Cl^- ions into the lattice of β-CD crystal. This supposition is tenable only on the assumption that the presence of β-CD in aqueous solution prohibits the formation of the close-packed structure of $CuCl_2$ in the process of crystal growth. To demonstrate this, a series of experiments were performed to measure structural changes of the interaction surface.

The comparison on surface features of β-CD, $CuCl_2 \cdot 2H_2O$, and $CuCl_2-\beta$-CD, as shown in Figure 3, gives a strong indication that the crystal growth patterns of the adduct particles are entirely different from that of either of the adducted components. Initially, β-CD, $CuCl_2 \cdot 2H_2O$, and $CuCl_2-\beta$-CD are structured like a regular hexagonal prism, a small stone, and a sheet metal piece, respectively. Next, grain sizes are different among the samples, but the distribution of the grain sizes is fairly uniform in each sample.

The tremendous difference in surface morphologies of these samples could be the result of different densities of stacking faults in solid phases of such samples. More importantly, the uniform size distribution and ordered spatial arrangement in the adducted state strongly imply a direct molecule-ion interaction between β-CD and Cu^{2+} as well as Cl^- ions.

The comparison of Raman spectra of β-CD, $CuCl_2 \cdot 2H_2O$, and $CuCl_2-\beta$-CD provides the most compelling evidence for a central role of β-CD in the formation of the

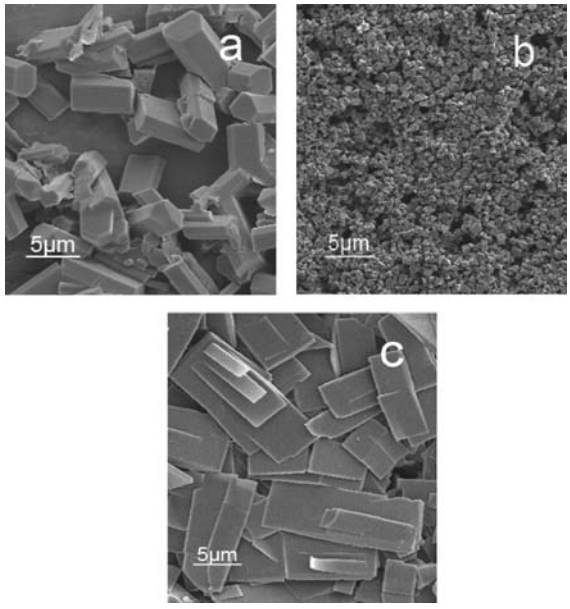

Figure 3. FE-SEM images of β-CD (a), $CuCl_2 \cdot 2H_2O$ (b), and $CuCl_2-\beta$-CD (c).

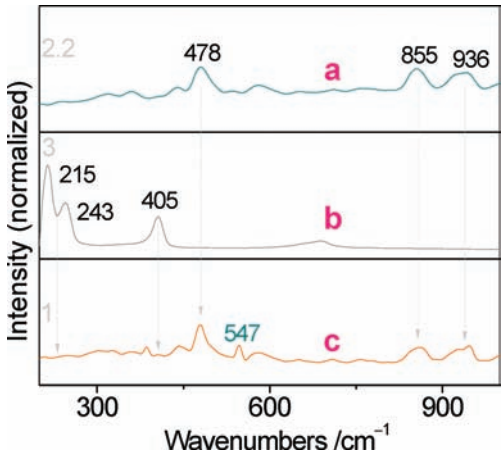

Figure 4. Raman spectra of β-CD (a), $CuCl_2 \cdot 2H_2O$ (b), and $CuCl_2-\beta$-CD (c). Relative signal intensity was normalized to the intensity of the peak at 478 cm^{-1} in curve c.

adduct. As seen in Figure 4, the bands of Cu−Cl (215 and 243 cm^{-1}) and Cu−O (405 cm^{-1})[32] in $CuCl_2 \cdot 2H_2O$ completely disappear, but those bands of β-CD at 478 (molecular skeletal vibration), 855 (ρ_{C-H}), and 936 (ν_{C-C})[33] cm^{-1} still remain at the similar positions in the case of $CuCl_2-\beta$-CD.

This interaction between β-CD and Cu^{2+} ions is confirmed by the presence of a stretching vibration band of Cu−O[34] at 547 cm^{-1} in the case of the adduct (see Figure 4c). We consider that the relatively large size, many hydrophilic groups, and rigid structure of β-CD molecules make it likely that they will have unusual properties to reduce the strength of the ionic bonding in $CuCl_2 \cdot 2H_2O$ by hydrogen bonding to the Cl^- ions or molecule-ion interaction to the Cu^{2+} ion, thereby causing

(31) Han, M. S.; Lee, B. G.; Ahn, B. S.; Moon, D. J.; Hong, S. I. *App. Surf. Sci.* **2003**, *211*, 76–81.
(32) Kakiuchi, M.; Abe, T.; Nakayama, H. *Geochem. J.* **2001**, *35*, 285–293.
(33) Blanch, G. P.; Castillo, M. L. R.; Caja, M. M.; Perez-Mendez, M.; Sanchez-Cortes, S. *Food Chem.* **2007**, *105*, 1335–1341.
(34) Kendix, E.; Moscardi, G.; Mazzeo, R.; Baraldi, P.; Prati, S.; Joseph, E.; Capelli, S. *J. Raman Spectrosc.* **2008**, *39*, 1104–1112.

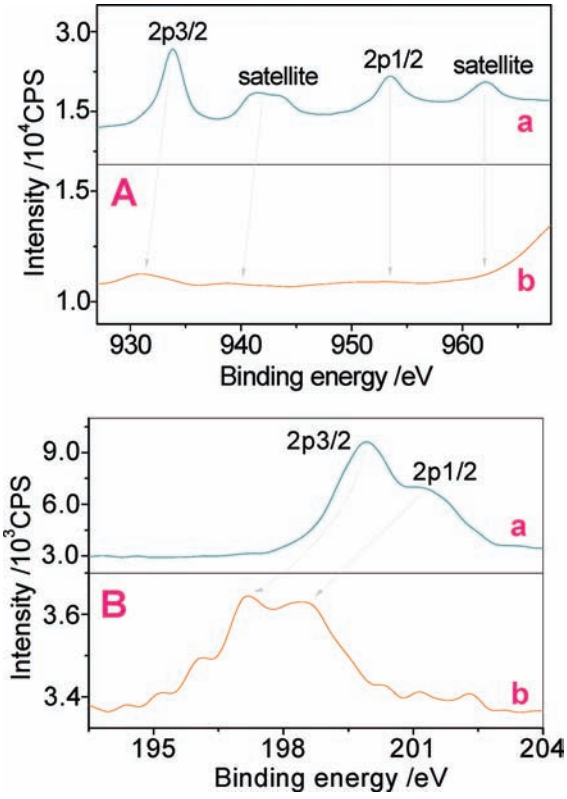

Figure 5. (A) XPS-(Cu_{2p}) and (B) XPS-(Cl_{2p}) spectra of $CuCl_2 \cdot 2H_2O$ (a) and $CuCl_2-\beta$-CD (b).

a separation between Cu^{2+} and Cl^- ions in the process of crystal growth. XRD and FE-SEM analyses have partly confirmed the effectiveness of the separation. Also, it can be further demonstrated by electronic structural analysis of Cu^{2+} and Cl^- ions.

Electronic Structural Analysis. XPS technique can be used to quantify the atoms at the sample surface.[35] Figure 5 depicts the XPS profiles of Cu 2p and Cl 2p in $CuCl_2 \cdot 2H_2O$ and $CuCl_2-\beta$-CD. Clearly, the XPS pattern of the $CuCl_2 \cdot 2H_2O$ presents the peaks of Cu 2p3/2 at the binding energies of 933.8 eV and Cu 2p1/2 at 953.4 eV, which are the same with those reported in the literature.[36,37] Their satellite peaks are observed at 942.5 and 962.2 eV, respectively. However, the binding energy of Cu 2p3/2 in $CuCl_2-\beta$-CD becomes 930.7 eV, which is lower than that before adduct by 3.1 eV, and the peak of Cu 2p1/2 as well as those satellite peaks nearly disappears in this case. At the same time, the peaks of Cl 2p3/2 and Cl 2p1/2 at the binding energies of 199.9 and 201.2 eV in the $CuCl_2 \cdot 2H_2O$ have shifted to 197.2 and 198.5 eV in the $CuCl_2-\beta$-CD, respectively.

The significant changes in the same direction are surprising and unexpected. This fact may reflect two points: (1) that the Cu−Cl bonds were weakened because of the adduct interaction, leading to an increase in the electron density of Cl^- ions, and (2) that the electron density of Cu^{2+} is enhanced by the contribution from the O atoms of

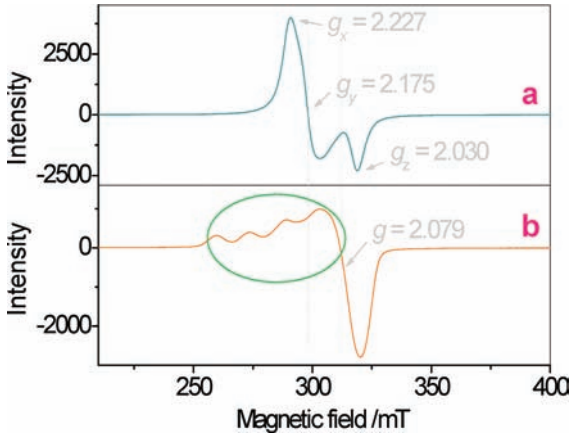

Figure 6. ESR spectra of $CuCl_2 \cdot 2H_2O$ (a) and $CuCl_2-\beta$-CD (b).

β-CD. Therefore, the result of XPS analysis indicates that the electronic structures of Cu^{2+} and Cl^- ions upon adduct have experienced a substantial transformation. This phenomenon, together with XRD, FE-SEM, and Raman analyses, provides a reasonable explanation for the alteration in ionic distribution pattern of the powder samples ($CuCl_2$ and its adduct) and gives a rare glimpse of the interplay between the electrostatic interaction between Cu^{2+} and Cl^- ions and the molecule-ion interaction between β-CD and these ions. Such a difference in electron structure of Cu^{2+} ions before and after adduct is verified by ESR analysis.

Figure 6 exhibits the ESR curves of $CuCl_2 \cdot 2H_2O$ and $CuCl_2-\beta$-CD. The coupling interaction among free Cu^{2+} ions in $CuCl_2 \cdot 2H_2O$ leads to the disappearance of hyperfine splitting from Figure 6a ($g_x = 2.227$, $g_y = 2.175$, and $g_z = 2.030$). However, the hyperfine splitting is clearly seen in the $CuCl_2-\beta$-CD ($g = 2.079$, Figure 6b), which is attributed to the electron spin−nuclear spin interaction.[37,38] The occurrence of such a situation is rare. It can be explained as the separation between Cu^{2+} ions to a larger extent in a $CuCl_2-\beta$-CD crystal than in $CuCl_2 \cdot 2H_2O$.

Actually, the change of ESR sign position or the change of g values is a reflection of the nature of chemical bonds. On the basis of the result of Figure 6, we predict that a weak molecule-ion interaction between inorganic ions and β-CD could decrease dramatically the electrostatic interaction between inorganic ions. The interesting structural change stimulates us to further investigate what the relation is between the structural change of adducted components and their thermal stabilities.

Unique Release Characteristics of Water. Figure 7 displays TG/DTG profiles reflecting decomposition processes of β-CD before and after adduct, from which the residual mass (RM, %) and the mass loss rate (V, %/sec) of the samples at different heating temperatures are obtained.

For $CuCl_2 \cdot 2H_2O$, the mass loss of 21.87% in the 330−402 K range is due to the release of crystal water molecules (calcd. 2.09). The decomposition of β-CD can be expressed in the following process: the first mass loss of 10.81% in the 326−380 K range is assigned to adsorbed water, and the other mass loss of 70.15%, between 542 and 649 K, is ascribed to the sharp decomposition of β-CD.

(35) Rodriguez-Arguelles, M. C.; Villalonga, R.; Serra, C.; Cao, R.; Sanroman, M. A.; Longo, M. A. *J. Colloid Interface Sci.* **2010**, *348*, 96–100.
(36) Park, M.; Choi, C. L.; Seo, Y. J.; Yeo, S. K.; Choi, J.; Komarneni, S.; Lee, J. H. *Appl. Clay Sci.* **2007**, *37*, 143–148.
(37) Figueiredo, R. T.; Martinez, A.; Granados, M. L.; Fierro, J. L. G. *J. Catal.* **1998**, *178*, 146–152.
(38) Kripal, R.; Yadav, M. P.; Govind, H. *Mol. Phys.* **2009**, *107*, 1555–1562.

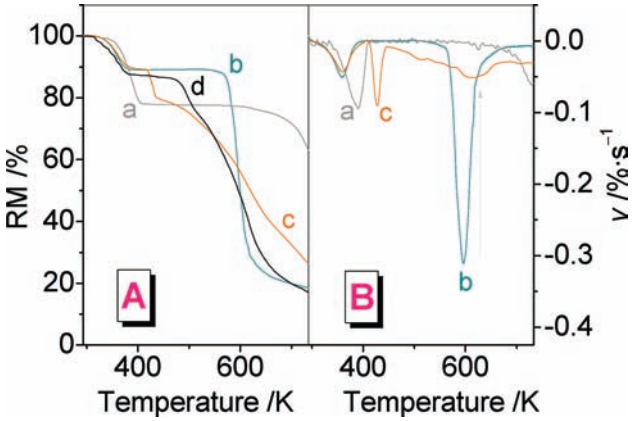

Figure 7. TG (A) and DTG (B) profiles of $CuCl_2 \cdot 2H_2O$ (a), β-CD (b), $CuCl_2-\beta$-CD (c), and the physical mixture (d).

However, process analysis shows that two independent signals (see Figure 7A) exist in the process of water release of the $CuCl_2-\beta$-CD. In the light of calculations, the first mass loss (10.66%, corresponding to 9.40 H_2O) from 335.0 to 383.5 K is larger than the second (9.38%, corresponding to 8.27 H_2O) from 420.8 to 435.3 K.

This result provides two important conclusions. First, water molecules exist in two kinds of forms, and one form is more stable than the other. Second, the adduct behavior leads to a strong and efficient way of changing the hydrate character of the adducted components: $CuCl_2 \cdot 2H_2O$ and β-CD. Taken together, we infer that the molecule-ion interaction has resulted in a regular distribution of Cu^{2+} and Cl^- ions as well as β-CD within aggregations, because the increase in the number of crystal water molecules is an important symbol that the ionic bond between Cu^{2+} and Cl^- ions is either broken or weakened to a great extent. The comparison between curves c and d in Figure 7A reveals that the simply physical mixing behavior in the solid state cannot achieve the same performance as the adduct behavior generated in solution. In addition, as seen in Figure 7B, the presence of the $CuCl_2 \cdot 2H_2O$ markedly decreases the maximum decomposition rate of the adducted β-CD.

Interesting Decomposition Products. The relative abundance (RA, %) in total ion current (TIC) curves of β-CD and $CuCl_2-\beta$-CD under the same heating conditions is shown in Figure 8. There is a double peak at 25.63 and 27.23 min in free β-CD, attributed to the rapid decomposition. Nevertheless, a small peak at 10.19 and a moderate peak at 17.34 min occur at earlier stages in the case of $CuCl_2-\beta$-CD. Further, the appearance of four release signals in Figure 8b implies that there is a significant change in thermal stability. The change is estimated based on products of decomposition at each peak time point. Figure 9 illustrates the mass spectra of $CuCl_2-\beta$-CD at four decomposition points (10.19, 17.34, 25.45, and 31.62 min), corresponding to the peak values in the TIC curve b.

The spectrum at the first decomposition point (10.19 min, 463.0 K, Figure 9a) gives strong release signals at m/z 18.010 (H_2O^+, 64.64%) and 35.976 (HCl^+, base peak), and a weak signal at m/z 43.989 (CO_2^+, 8.41%). This suggests that the adducted $CuCl_2$ decomposes more than β-CD even at such a low temperature.

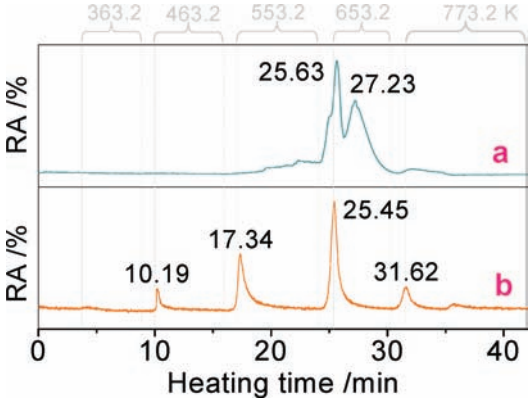

Figure 8. TIC curves of β-CD (a) and $CuCl_2-\beta$-CD (b).

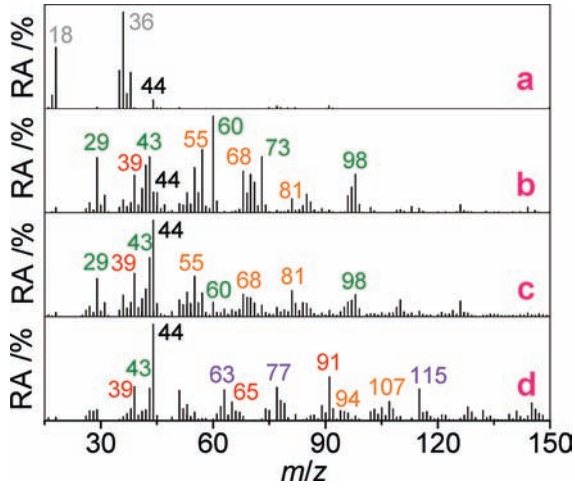

Figure 9. Mass spectra of $CuCl_2-\beta$-CD at 10.19 (a), 17.34 (b), 25.45 (c), and 31.62 min (d).

Figures 9b (17.34 min, 553.2 K) and c (25.45 min, 653.2 K) present strong signals at m/z 29.003 (CHO^+), 43.019 ($C_2H_3O^+$), 44.026 (CO_2^+), 60.021 ($C_2H_4O_2^+$), 73.029 ($C_3H_5O_2^+$), and 98.037 ($C_5H_6O_2^+$), resulting from the decomposition of β-CD.[30] According to the number and type of the fragments released at 17.34 min, we deduce that the decomposition of the adducted β-CD is earlier than that of free β-CD.

The spectrum at the final decomposition point (31.62 min, 773.2 K) exhibits many different features from other decomposition points. For instance, several bigger fragments at m/z 63.024 ($C_5H_3^+$, 31.58%), 77.039 ($C_6H_5^+$, 34.31%), 91.055 ($C_7H_7^+$, 41.32%), and 115.055 ($C_9H_7^+$, 32.73%) appear at the moment in higher RA values. This completely differs from the effects of Li_2CO_3, $NaAsO_2$, and $(NH_4)_6Mo_7O_{24} \cdot 4H_2O$ on β-CD at this stage.[27−29]

Upon inspection of each of the features, there are two interesting phenomena. (1) The glucopyranose ring of β-CD in the presence of $CuCl_2 \cdot 2H_2O$ is easily transformed into a series of tropylium ions: $C_3H_3^+$ (39.023, 35.29%), $C_5H_5^+$ (65.039, 19.26%), and $C_7H_7^+$ (91.055, 45.32%). The presence of the series of tropylium ions is similar to the result obtained for Li_2CO_3 stimulation,[27] but the three- and seven-membered cyclic tropylium ions are prone to be formed in higher RA values at lower and higher temperatures, respectively, in comparison with the case of $Li_2CO_3-\beta$-CD. (2) The series of molecular ions

$C_3H_3O^+$ (55.018), $C_4H_4O^+$ (68.027), $C_5H_5O^+$ (81.034), and $C_7H_7O^+$ (107.047) are present in the mass spectra simultaneously, which were not observed in previous experiments because of their rarity. The chemistry of the small molecular ions, each having the same number of carbon and hydrogen atoms, has received much interest in the past.[39−43]

One of the most difficult problems in mass spectrometric microanalysis is the assignment of structures to the individual isomers. According to calculations made by Qu and his colleagues, the $C_3H_2OH^+$ hydroxyl tropylium ion is the most thermally stable of all its 22 isomers and 34 interconversion transition states.[39] Also, it has been reported that $C_4H_4O^+$ ions mainly have the furan radical ion structure in the past few decades.[41] Although the work of Alzueta and his collaborator showed that C_5H_5O and C_5H_4OH dissociate fairly rapidly, while C_5H_5OH and C_5H_4O are thermally more stable,[42] this situation does not seem to occur in view of the result of Figure 9. Presumably, the $C_5H_5O^+$ ion is probably a pyran ring structure, on the basis of reported data,[44,45] or more likely the $C_5H_4OH^+$ hydroxyl tropylium ion since the $C_5H_5^+$ tropylium ion has been observed in the same system under similar conditions. There have been few reports concerning the assignment of structures to $C_7H_6OH^+$ ions resulting from the degradation of carbohydrates. Nevertheless, the structural transformation among the tropylium ions $C_3H_3^+$, $C_5H_5^+$, and $C_7H_7^+$ has been reported.[27,46,47] This allows us to consider the presence of a similar transition among the hydroxyl tropylium ions proposed.

All together, we tentatively speculate that such a series of fragments are likely to be a group of hydroxyl tropylium ions (see Figure 10), in considering the glucopyranose ring conformation of β-CD. Actually, they cannot be directly obtained by simple cleavage of chemical bonds in a β-CD molecule, but instead as a result of a molecular rearrangement.

The mechanisms describing the rupture of 1,4-glycosidic bonds are related to the interaction between Cu^{2+} ions and oxygen atoms, probably as well as the interaction between Cl^- ions and hydrogen atoms. The hypothesis of such a direct interaction has been supported by XPS analysis of the sample.

Formation of CuCl Crystal. Sintering experiments in air were done to estimate the relationship between the carbonization of β-CD and the reduction of Cu^{2+} ions. Table 1 summarizes the result of sintering measurements of β-CD, $CuCl_2 \cdot 2H_2O$ and $CuCl_2-\beta$-CD at different temperatures in air. The residual mass percentage (RMP, %) of each sample is determined by a ratio of the residual mass of the sample at higher temperatures to its residual mass at 333.2 K.

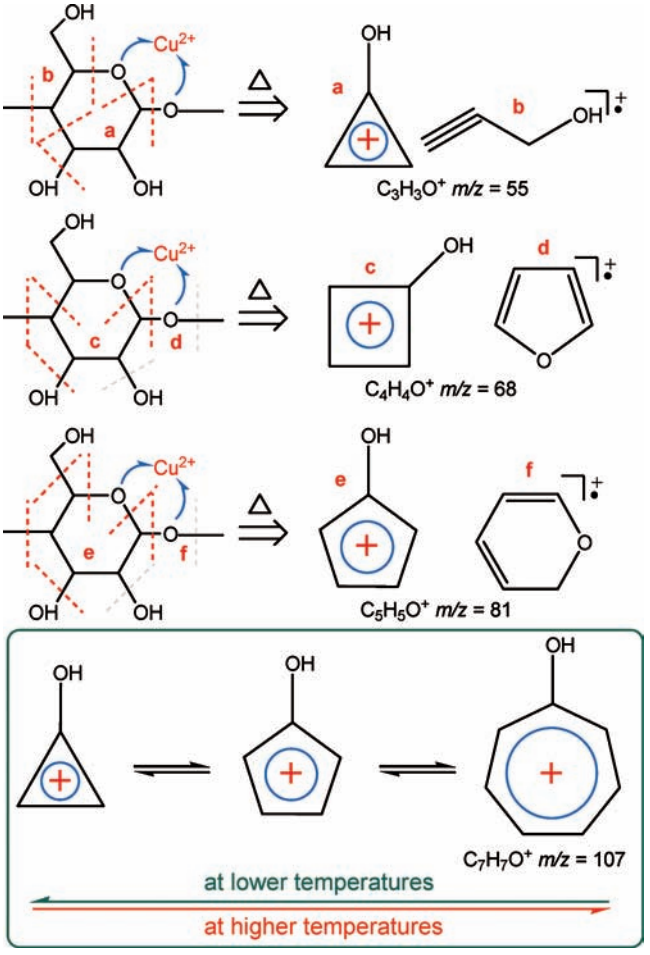

Figure 10. Proposed formation mechanisms concerning the series of hydroxyl tropylium ions.

Table 1. RMP Values of β-CD, $CuCl_2 \cdot 2H_2O$, and $CuCl_2-\beta$-CD at Different Temperatures in Air

	RMP (%) at different temperatures (K)				
samples	523.2	573.2	623.2	673.2	723.2
β-CD	94.22	56.05	43.01	25.52	1.21
$CuCl_2 \cdot 2H_2O$	82.53	81.80	79.82	76.64	65.80
$CuCl_2-\beta$-CD	74.47	8.20	6.31	5.24	3.13

From the table, we see that the RMP values of free $CuCl_2 \cdot 2H_2O$ do not change greatly from 523.3 to 623.2 K, and free β-CD loses most of its RMP value in the same temperature interval. However, the $CuCl_2-\beta$-CD decomposes almost completely at 573.2 K or lower. In fact, the present data give a hint that the existence of $CuCl_2 \cdot 2H_2O$ accelerates the decomposition of β-CD in air, and vice versa. At the same time it stimulates us to explore what reasons there may be for such a response.

Figure 11 shows the XRD pattern of the sintered $CuCl_2-\beta$-CD at 573.2 K in air. The three characteristic diffraction peaks at 2θ angles of 28.6, 47.5, and 56.2°, are assigned as the (111), (220), and (311) phases of crystal structure of cuprous chloride (CuCl), respectively, according to the XRD database (JCPDS no. 27-0184). The formation of CuCl crystal is attributed to the reduction of carbon,

(39) Qu, Z. W.; Ding, Y. H.; Li, Z. S. *J. Mol. Struct.* **1999**, *489*, 195–208.
(40) Shu, J.; Peterka, D. S.; Leone, S. R.; Ahmed, M. *J. Phys. Chem. A* **2004**, *108*, 7895–7902.
(41) Yan, S. H.; Bu, Y. X.; Sun, L. X. *J. Mol. Struct.* **2004**, *671*, 161–172.
(42) Alzueta, M. U.; Glarborg, P.; Dam-Johansen, K. *Int. J. Chem. Kinet.* **2000**, *32*, 498–522.
(43) Solano, E.; Stashenko, E.; Martinez, J.; Mora, U.; Kouznetsov, V. *J. Mol. Struct-Theochem.* **2006**, *769*, 83–85.
(44) Espinoza, E. A. S.; Narvaez, W. E. V. *J. Mass Spectrom.* **2009**, *44*, 1452–1458.
(45) Espinoza, E. A. S.; Narvaez, W. E. V. *J. Mass Spectrom.* **2010**, *45*, 722–733.
(46) Moini, M. *J. Am. Soc. Mass Spectrom.* **1992**, *3*, 631–636.
(47) Feng, J.; Leszczynski, J.; Weiner, B.; Zerner, M. C. *J. Am. Chem. Soc.* **1989**, *111*, 4648–4655.

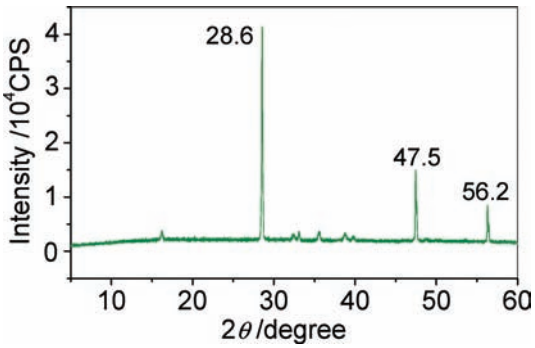

Figure 11. XRD pattern of the sintered $CuCl_2-\beta$-CD.

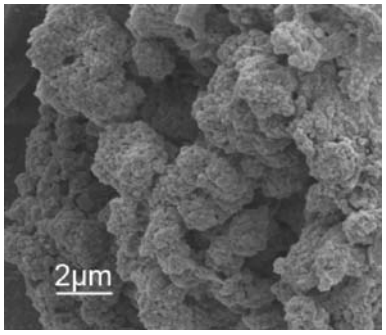

Figure 12. FE-SEM image of the sintered $CuCl_2-\beta$-CD.

which comes from the process of carbonizing β-CD, to $CuCl_2$. In this case, the reduction reaction proceeds very cleanly (checked by the figure) and no side reaction products such as Cu are observed.

CuCl crystal has attracted a significant degree of experimental attention for its unusual electrical and optical properties.[48−50] It is interesting and unexpected that the reduction from $CuCl_2$ to CuCl occurs at a lower temperature in the process of carbonization of β-CD. As seen from Figure 12, the bulk CuCl crystal has a well-defined coralline-like macroporous structure.

Raman spectrum of the sintered $CuCl_2-\beta$-CD at 573.2 K in air in Figure 13 gives two pronounced signals at 1374.4 and 1589.6 cm^{-1}, suggesting the occurrence of the D and G bands of the C−C vibration of graphite carbon,[51−53] This signifies the formation of the carbon material with an sp^2 orbital structure. Undoubtedly, the reduction of $CuCl_2$ is involved in the generation of the carbon atoms.

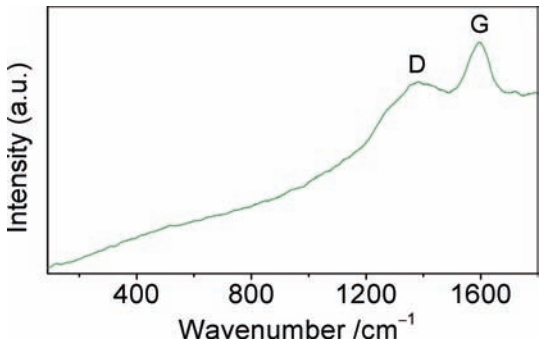

Figure 13. Raman spectrum of the sintered $CuCl_2-\beta$-CD.

According to the comparison between Figures 11 and 13, we infer that the CuCl crystal is the main product in the sintering operation (see eq 1), because there are no observable peaks in the XRD spectrum attributable to graphite carbon.

$$4CuCl_2 + C + 2H_2O \xrightarrow{573.2K} 4CuCl + 4HCl\uparrow + CO_2\uparrow \quad (1)$$

Further, the relative intensity ratio of D- to G-band is a key factor to determine a graphitic structure. Herein, the intensity ratio of the two Raman peaks is calculated to be 0.87, which is indicative of an amorphous carbon structure with a high content of lattice edges and plane defects.[54−56]

All the results emphasize the importance of the effect of the adduct interaction between $CuCl_2$ and β-CD on the electrostatic interaction between Cu^{2+} and Cl^- ions.

Conclusions

The present study demonstrates that the presence of β-CD molecules weakens the strength of ionic bonds in $CuCl_2$ by molecule-ion interaction to the Cu^{2+} and Cl^- ions by microstructural analysis, especially electronic structural analysis. Several interesting phenomena, such as the unique release characteristics of water, the generation of a series of hydroxyl tropylium ions, and the formation of CuCl crystal and graphite carbon, occur in the process of thermal decomposition of $CuCl_2-\beta$-CD. We believe that this study provides a basis for further work in this area, which is helpful to establish a link between supramolecular chemistry and inorganic chemistry.

Acknowledgment. This project was supported by NSFC (No. 21071139) and Natural Science Foundation of Anhui Province (No. 090416228).

(48) Lucas, F. O.; McNally, P. J.; Daniels, S.; Taylor, D. M. *J. Mater. Sci.: Mater. Electron.* **2009**, *20*, 144–148.
(49) Gavrilyuk, A. I. *Sol. Energy Mater. Sol. Cells* **2010**, *94*, 515–523.
(50) Danieluk, D.; Bradley, A. L.; Mitra, A.; O'Reilly, L.; Lucas, O. F.; Cowley, A.; McNally, P. J.; Foy, B.; McGlynm, E. *J. Mater. Sci.: Mater. Electron.* **2009**, *20*, 76–80.
(51) Calizo, I.; Balandin, A. A.; Bao, W.; Miao, F.; Lau, C. N. *Nano Lett.* **2007**, *7*, 2645–2649.
(52) Kudin, K. N.; Ozbas, B.; Schniepp, H. C.; Rrud'homme, R. K.; Aksay, I. A.; Car, R. *Nano Lett.* **2008**, *8*, 36–41.
(53) Graf, D.; Molitor, F.; Ensslin, K.; Stampfer, C.; Jungen, A.; Hierold, C.; Wirtz, L. *Nano Lett.* **2007**, *7*, 238–242.
(54) Subrahmanyam, K. S.; Manna, A. K.; Pati, S. K.; Rao, C. N. R. *Chem. Phys. Lett.* **2010**, *497*, 70–75.
(55) Tommasini, M.; Castiglioni, C.; Zerbi, G. *Phys. Chem. Chem. Phys.* **2009**, *11*, 10185–10194.
(56) Castiglioni, C.; Negri, F.; Rigolio, M.; Zerbi, G. *J. Chem. Phys.* **2001**, *115*, 3769–3778.